

**FABRICATION AND CHARACTERIZATION OF  
CARBONATE APATITE SCAFFOLDS COATED  
WITH ALGINATE AND GELATIN**

**FADILAH BINTI MOHD DARUS**

**UNIVERSITI SAINS MALAYSIA**

**2019**

**FABRICATION AND CHARACTERIZATION OF CARBONATE APATITE  
SCAFFOLDS COATED WITH ALGINATE AND GELATIN**

**by**

**FADILAH BINTI MOHD DARUS**

**Thesis submitted in fulfillment of the  
requirements for the degree of  
Master of Science**

**April 2019**

## ACKNOWLEDGEMENT

In the name of Allah, the Most Gracious and the Most Merciful. First and foremost, I would like to express my gratitude to Allah SWT for His blessing and strength given to me to finish the project and complete my thesis.

First of all, I would like to thank the School of Materials and Minerals Resources Engineering, USM for providing me space and good facilities during my studies here. Besides that, I would like to offer my gratitude to my supervisor, Prof. Ir. Dr. Mariatti Jaafar for her continuous supervision, inspiration, patience and valuable time in guiding me throughout the entire duration to complete this research work. My sincere appreciation also to give to my co-supervisor, Dr. Nurazreena Bt. Ahmad for their constructive input in this project.

Not to forget, I must extend my appreciation to all the administrative and technical staff in this faculty for their assistance and technical support in operating machines during my research. Besides that, I would like to take this opportunity to dedicate my appreciation to my supported team members and fellow friends, who helped me, supported me and gave me strength in completing this project.

Warmest appreciation to my mother, Rojmah Bt. Taib and my beloved siblings for their endless love, support, and encouragement. I am also indebted to every individual for their involvement directly or indirectly throughout this project. May Allah SWT return your kindness.

Finally, I would also like to acknowledge the financial support from the Ministry of Higher Education Malaysia through MyMaster scheme (MyBrain15) as well as TRGS grant (No: 6761004).

## TABLE OF CONTENTS

	<b>Page</b>
<b>ACKNOWLEDGEMENT.....</b>	<b>ii</b>
<b>TABLE OF CONTENTS.....</b>	<b>iii</b>
<b>LIST OF TABLES.....</b>	<b>vii</b>
<b>LIST OF FIGURES.....</b>	<b>viii</b>
<b>LIST OF ABBREVIATIONS.....</b>	<b>xiii</b>
<b>LIST OF SYMBOLS.....</b>	<b>xiv</b>
<b>ABSTRAK.....</b>	<b>xv</b>
<b>ABSTRACT.....</b>	<b>xvi</b>
<b>CHAPTER 1 INTRODUCTION.....</b>	<b>1</b>
1.1 Background of study.....	1
1.2 Problem statement.....	3
1.3 Objectives.....	5
1.4 Organization of thesis.....	6
<b>CHAPTER 2 LITERATURE REVIEW.....</b>	<b>8</b>
2.1 Introduction.....	8
2.2 Tissue engineering.....	8
2.3 Overview of bone graft.....	9
2.4 Carbonate apatite bone replacement.....	13
2.4.1 Hydrothermal treatment.....	14
2.4.2 Carbonation and phosphorization.....	18
2.5 Bioceramic scaffold.....	18
2.6 Bioceramic scaffolds with natural polymer coating.....	25
2.6.1 Coating with alginate.....	26
2.6.2 Coating with gelatin.....	27
2.7 Surface treatment of bioceramics scaffold.....	29
2.8 Bioactivity evaluation.....	31
2.9 Summary.....	33
<b>CHAPTER 3 METHODOLOGY.....</b>	<b>35</b>
3.1 Introduction.....	35
3.2 Materials.....	35

3.2.1	$\beta$ -tricalcium phosphate.....	35
3.2.2	Polyvinyl alcohol.....	36
3.2.3	Poly (methyl methacrylate).....	36
3.2.4	Hydrogen peroxide.....	37
3.2.5	Sodium hydrogen carbonate.....	37
3.2.6	Sodium carbonate.....	37
3.2.7	Sodium alginate.....	37
3.2.8	Bovine gelatin.....	38
3.2.9	3-(trimethoxysilyl) propyl methacrylate.....	38
3.2.10	Glutaraldehyde.....	38
3.2.11	Hanks' balanced salt solution.....	39
3.2.12	Methanol.....	39
3.3	Experimental methods.....	40
3.3.1	Fabrication of CO <sub>3</sub> Ap scaffold.....	40
	3.3.1(a) Fabrication of $\beta$ -TCP scaffold.....	40
	3.3.1(b) Phase transformation reaction.....	41
3.3.2	Natural polymer coating.....	43
	3.3.2(a) Sodium alginate coating.....	43
	3.3.2(b) Bovine gelatin coating.....	44
3.3.3	Silane treated CO <sub>3</sub> Ap scaffold.....	46
3.3.4	Bioactivity evaluation.....	46
3.4	Characterization techniques.....	47
3.4.1	X-ray diffraction (XRD).....	47
3.4.2	Fourier transform infra-red (FTIR) spectroscopy.....	47
3.4.3	Carbon hydrogen nitrogen (CHN) analyzer.....	48
3.4.4	Field emission scanning electron microscope (FESEM).....	48
3.4.5	Porosity measurement.....	49
3.4.6	Natural polymer content.....	49
3.4.7	Viscosity measurement.....	49
3.4.8	Compression test.....	50
3.4.9	Inductive coupled plasma-optical emission spectroscopy (ICP-OES).....	50

<b>CHAPTER 4</b>	<b>RESULTS AND DISCUSSION.....</b>	<b>51</b>
4.1	Introduction.....	51
4.2	Raw materials characterization.....	51
4.2.1	$\beta$ -TCP powder.....	52
	4.2.1(a) Structural analysis.....	52
	4.2.1(b) Analytical analysis.....	54
4.2.2	Natural polymer.....	54
4.3	Fabrication of CO <sub>3</sub> Ap scaffold.....	57
4.3.1	Morphological analysis of scaffold before and after hydrothermal treatment.....	57
4.3.2	Structural analysis of scaffold before and after hydrothermal treatment.....	65
4.3.3	Analytical analysis of scaffold before and after hydrothermal treatment.....	68
4.3.4	Elemental analysis of scaffold before and after Hydrothermal treatment.....	70
4.3.5	Compressive strength of scaffold before and after hydrothermal treatment.....	72
4.4	Natural polymer coating.....	75
4.4.1	Characterization of CO <sub>3</sub> Ap scaffold coated with sodium alginate.....	75
	4.4.1(a) Scaffold morphology and content of sodium alginate.....	76
	4.4.1(b) Compressive strength and porosity.....	78
	4.4.1(c) Analytical properties.....	80
4.4.2	Characterization of CO <sub>3</sub> Ap scaffold coated with bovine gelatin.....	82
	4.4.2(a) Scaffold morphology and content of bovine gelatin.....	82
	4.4.2(b) Compressive strength and porosity.....	84
	4.4.2(c) Analytical properties.....	87
4.5	Silane treated CO <sub>3</sub> Ap scaffold.....	88
4.5.1	Compressive strength and porosity.....	88

4.5.2	Morphological analysis.....	90
4.5.3	Analytical properties.....	92
4.6	Bioactivity evaluation.....	95

**CHAPTER 5 CONCLUSION AND FUTURE COMMENDATIONS.....99**

5.1	Conclusion.....	99
5.2	Recommendations for future research.....	101

**REFERENCES.....102**

**APPENDICES**

APPENDIX A: CALCULATION FOR THE CO<sub>3</sub><sup>2-</sup> ION CONTENT

**LIST OF PUBLICATIONS**

## LIST OF TABLES

	<b>Page</b>
Table 2.1	Comparison of A-type and B-type of CO <sub>3</sub> Ap.....14
Table 2.2	Types of precursor used in the fabrication of CO <sub>3</sub> Ap scaffold by hydrothermal treatment.....15
Table 3.1	General properties of $\beta$ -TCP powders.....36
Table 3.2	General properties of PVA.....36
Table 3.3	General properties of H <sub>2</sub> O <sub>2</sub> liquids.....37
Table 3.4	General properties of MTMS.....38
Table 3.5	General properties of GA.....39
Table 3.6	General properties of methanol.....39
Table 3.7	Sample designation of CO <sub>3</sub> Ap with different concentration and polymer coating.....43
Table 4.1	Ca, P and molar Ca/P ratio of $\beta$ -TCP scaffold after hydrothermal treatment in NaHCO <sub>3</sub> and Na <sub>2</sub> CO <sub>3</sub> aqueous solutions.....71
Table 4.2	Average pore size and porosity of $\beta$ -TCP scaffold after hydrothermal treatment in NaHCO <sub>3</sub> and Na <sub>2</sub> CO <sub>3</sub> aqueous solutions.....75
Table 4.3	Sodium alginate content on the CO <sub>3</sub> Ap scaffold after coating process.....78
Table 4.4	Bovine gelatin content on the CO <sub>3</sub> Ap scaffold after coating process.....84
Table 4.5	Porosity of untreated and treated CO <sub>3</sub> Ap scaffolds.....90
Table 4.6	Polymer content on the CO <sub>3</sub> Ap scaffold.....92

## LIST OF FIGURES

	<b>Page</b>
Figure 2.1	General concept of tissue engineering process.....9
Figure 2.2	Concept of bone regeneration by bone scaffold substitute.....12
Figure 2.3	Evolution of bone graft substitute materials.....13
Figure 2.4	Scanning Electron Microscopy (SEM) image of $\alpha$ -TCP foam after immersion in 4 mol/L $\text{Na}_2\text{CO}_3$ .....16
Figure 2.5	Mechanisms of dissolution-precipitation ions.....17
Figure 2.6	Schematic diagram of the polymeric sponge method.....22
Figure 2.7	Schematic diagram of the direct foaming method.....22
Figure 2.8	Schematic diagram of the gel-casting process.....23
Figure 2.9	The polymer solution dipping method developed to coat bioceramic scaffolds with a biodegradable polymer.....26
Figure 2.10	Mechanisms of glutaraldehyde reaction with amine groups on gelatin to form cross-links.....28
Figure 2.11	Schematic diagram of PLGA scaffolds before and after coated with gelatin.....29
Figure 2.12	Scheme of trialkoxy silane reaction with a surface.....30
Figure 2.13	Schematic presentations of the origin of negative charge on the HAp surface and the process of bonelike apatite formation thereon in SBF.....32
Figure 2.14	SEM images showing apatite formation on the surfaces of GCG coated BG scaffolds after immersion in SBF for (a) and (b) 3 days and (c) and (d) 7 days.....33
Figure 3.1	Sintering profile of $\beta$ -TCP scaffolds.....41

Figure 3.2	Schematic diagrams on (a) Fabrication of $\beta$ -TCP scaffold and (b) Phase transformation reaction.....	42
Figure 3.3	Overall flowchart of coating process.....	45
Figure 4.1	XRD pattern of $\beta$ -TCP powder.....	52
Figure 4.2	FTIR spectrum of $\beta$ -TCP powder. ....	53
Figure 4.3	Molecular structure of $\beta$ -TCP powder.....	54
Figure 4.4	FTIR spectrum of sodium alginate powder.....	55
Figure 4.5	Molecular structure of sodium alginate.....	55
Figure 4.6	FTIR spectrum of bovine gelatin powder... ..	56
Figure 4.7	Molecular structure of bovine gelatin.....	57
Figure 4.8	$\beta$ -TCP scaffold fabricated by a combination method of direct foaming and sacrificial template, (a) Photograph of $\beta$ -TCP scaffold and micrograph of $\beta$ -TCP scaffold cross-sectional at (b) 60 x magnification and (c) 1000 x magnification.....	58
Figure 4.9	Distribution graph of (a) macropores and (b) micropores.....	59
Figure 4.10	Morphology of $\beta$ -TCP scaffold after hydrothermal treatment with 2 mol/L NaHCO <sub>3</sub> solution at 200°C for various soaking time: (a) 2, (c) 4, (e) 6, (g) 8 (d) and (i) 10 days observed at 100 x, (b), (d), (f), (h) and (j) observed at 1000 x magnification.....	62
Figure 4.11	Morphology of $\beta$ -TCP scaffold after hydrothermal treatment with 2 mol/L Na <sub>2</sub> CO <sub>3</sub> solution at 200°C for various soaking time: (a) 2, (c) 4, (e) 6, (g) 8 (d) and (i) 10 days observed at 100 x, (b), (d), (f), (h) and (j) observed at 1000 x magnification.....	63

Figure 4.12	XRD pattern of $\beta$ -TCP scaffold before and after hydrothermal reaction with 2 mol/L $\text{NaHCO}_3$ at 200°C with various soaking time.....	66
Figure 4.13	XRD pattern of $\beta$ -TCP scaffold before and after hydrothermal reaction with 2 mol/L $\text{Na}_2\text{CO}_3$ at 200°C with various soaking time.....	67
Figure 4.14	Conversion rates to $\text{CO}_3\text{Ap}$ as a function of time with different carbonate solutions.....	68
Figure 4.15	FTIR spectra of $\beta$ -TCP scaffold before and after hydrothermal reaction with 2 mol/L $\text{NaHCO}_3$ at 200°C with various soaking time.....	69
Figure 4.16	FTIR spectra of $\beta$ -TCP scaffold before and after hydrothermal reaction with 2 mol/L $\text{Na}_2\text{CO}_3$ at 200°C with various soaking time.....	70
Figure 4.17	Carbonate content (wt. %) in $\text{CO}_3\text{Ap}$ obtained by hydrothermal treatment of $\beta$ -TCP scaffold in $\text{NaHCO}_3$ and $\text{Na}_2\text{CO}_3$ aqueous solutions.....	72
Figure 4.18	Compression strengths of $\beta$ -TCP scaffold before and after hydrothermal treatment in $\text{NaHCO}_3$ and $\text{Na}_2\text{CO}_3$ aqueous solution.....	73
Figure 4.19	Morphology of $\beta$ -TCP scaffold after hydrothermal treatment (a) 6 days $\text{NaHCO}_3$ and (b) 8 days $\text{Na}_2\text{CO}_3$ at 5000 x magnification.....	74
Figure 4.20	Photograph of (a) $\text{CO}_3\text{Ap}$ scaffold before and (b - d) after coating with sodium alginate.....	76
Figure 4.21	Morphology of $\text{CO}_3\text{Ap}$ scaffold coated with sodium alginate; (a) 1SA- $\text{CO}_3\text{Ap}$ , (b) 3SA- $\text{CO}_3\text{Ap}$ and (c) 5SA- $\text{CO}_3\text{Ap}$ observed at 100x while (d), (e), and (f) observed at 1000x magnification.....	77

Figure 4.22	Percentage of porosity and compressive strength of CO <sub>3</sub> Ap scaffold before and after coating with different concentration of sodium alginate.....	80
Figure 4.23	FTIR spectra of (a) CO <sub>3</sub> Ap, (b) 1SA-CO <sub>3</sub> Ap, (c) 3SA-CO <sub>3</sub> Ap, (d) 5SA-CO <sub>3</sub> Ap scaffold and (e) SA.....	81
Figure 4.24	Photograph of (a) CO <sub>3</sub> Ap scaffold before and (b - d) after coating with bovine gelatin.....	82
Figure 4.25	Morphology of CO <sub>3</sub> Ap scaffold coated with bovine gelatin; (a) 1BG-CO <sub>3</sub> Ap, (b) 3BG-CO <sub>3</sub> Ap and (c) 5BG-CO <sub>3</sub> Ap observed at 100x while (d), (e), and (f) observed at 1000x magnification.....	83
Figure 4.26	Percentage of porosity and compressive strength of CO <sub>3</sub> Ap scaffold before and after coating with different concentration of bovine gelatin.....	86
Figure 4.27	FTIR spectra of CO <sub>3</sub> Ap, 1BG-CO <sub>3</sub> Ap, 3BG-CO <sub>3</sub> Ap, 5BG-CO <sub>3</sub> Ap scaffold and BG.....	87
Figure 4.28	Comparison of compressive strength between CO <sub>3</sub> Ap scaffold, 5SA-CO <sub>3</sub> Ap, 5BG-CO <sub>3</sub> Ap, and treated CO <sub>3</sub> Ap scaffold with silane solution.....	89
Figure 4.29	Morphology of (a) CO <sub>3</sub> Ap scaffold, (b) treated CO <sub>3</sub> Ap scaffold (c) treated CO <sub>3</sub> Ap scaffold and coated with 5 wt. % sodium alginate and (d) treated CO <sub>3</sub> Ap scaffold and coated with 5 wt. % bovine gelatin observed at 1000x magnification.....	91
Figure 4.30	FTIR spectrum for (a) untreated CO <sub>3</sub> Ap scaffold, (b) T-CO <sub>3</sub> Ap scaffold.....	93
Figure 4.31	FTIR spectrum for (a) 5SA-CO <sub>3</sub> Ap, (b) treated 5SA-CO <sub>3</sub> Ap, (c) 5BG-CO <sub>3</sub> Ap, and (d) treated 5BG-CO <sub>3</sub> Ap scaffold.....	95

Figure 4.32	Morphology of (a) CO <sub>3</sub> Ap scaffold (14 days) (b) CO <sub>3</sub> Ap scaffold (28 days), (c) treated 5SA-CO <sub>3</sub> Ap (14 days), (d) treated 5SA-CO <sub>3</sub> Ap (28 days), (e) treated 5BG-CO <sub>3</sub> Ap (14 days), and (f) treated 5BG-CO <sub>3</sub> Ap (28 days).....	97
Figure 4.33	Ca <sup>2+</sup> ions release from scaffold in HBSS for various immersion period.....	98
Figure 4.34	PO <sub>4</sub> <sup>3-</sup> ions release from scaffold in HBSS for various immersion period.....	98

## LIST OF ABBREVIATIONS

ASTM	American society for testing and materials
Ca	Calcium
CHN	Carbon hydrogen nitrogen
CPC	Calcium phosphate ceramic
DCM	Dimethyl carbonate
DCPA	Calcium hydrogen phosphate dehydrate
FESEM	Field emission scanning electron microscopy
FTIR	Fourier transform infra-red
GA	Glutaraldehyde
HAp	Hydroxyapatite
HBSS	Hanks' balanced salt solution
ICP-OES	Inductive coupled plasma-optical emission spectroscopy
ICSD	Inorganic crystal structure database
L/P	Liquid to powder ratio
min	Minute
MTMS	3-(trimethoxysilyl) propyl methacrylate
P	Phosphate
PDLLA	Poly (D, L-lactide)
PLGA	Poly (lactide-co-glycolide)
PMMA	Poly (methyl methacrylate)
PP	Polypropylene
PU	Polyurethane
PVA	Polyvinyl alcohol
rpm	Rotation per minute
TCP	Tricalcium phosphate
v/v	Volume per volume
XRD	X-ray diffraction
$\alpha$ -TCP	Alpha tricalcium phosphate
$\beta$ -TCP	Beta tricalcium phosphate

## LIST OF SYMBOLS

wt.	Weight
%	Percent
$\theta$	Theta
$^{\circ}\text{C}$	Degree celcius
$^{\circ}$	Degree
$\mu\text{m}$	Micrometer
mm	Milimeter
MPa	Mega pascal
kN	Kilo newton
g	Gram
g/mol	Gram per mole
mol/L	Mole per liter
$\approx$	Almost equal to
$>$	Greater than
$\geq$	Greater than or equal to
$\sim$	Approximately
$\lambda$	Wavelength
$\text{\AA}$	Angstrom
$^{\circ}\text{C}/\text{min}$	Degree celcius per minute
$\text{cm}^{-1}$	Reciprocal centimeter

# **FABRIKASI DAN PENCIRIAN PERANCAH APATIT KARBONAT DISALUT DENGAN ALGINAT DAN GELATIN**

## **ABSTRAK**

Apatit karbonat ( $\text{CO}_3\text{Ap}$ ) mendapat perhatian yang luas dalam bidang percantuman tulang kerana ia mempunyai komposisi kimia yang sama dengan tulang manusia. Walau bagaimanapun, penggantian tulang  $\text{CO}_3\text{Ap}$  masih belum dikomersialkan kerana kestabilan haba karbonat yang rendah pada suhu tinggi. Selain itu, semua bahan berliang mempunyai had kekurangan dari segi kekuatan kerana wujudnya liang. Tujuan kajian ini dijalankan ialah untuk menghasilkan perancah  $\text{CO}_3\text{Ap}$  menggunakan tindak balas penguraian ganda dua-pemendakan semasa rawatan hidroterma dan untuk meningkatkan kekuatan mampatan perancah dengan menggunakan salutan polimer asli. Kesan kedua-dua larutan yang berbeza, iaitu  $\text{NaHCO}_3$  dan  $\text{Na}_2\text{CO}_2$  terhadap perancah  $\beta$ -TCP telah dikenalpasti. Didapati perancah  $\text{CO}_3\text{Ap}$  dengan 8.95 wt. % kandungan karbonat berjaya dihasilkan menggunakan larutan  $\text{NaHCO}_3$ . Saiz purata liang perancah adalah kira-kira 180  $\mu\text{m}$  dengan 72 % keliangan. Purata kekuatan mampatan yang diperolehi dari perancah  $\text{CO}_3\text{Ap}$  ialah 0.7 MPa. Perancah  $\text{CO}_3\text{Ap}$  telah disalut dengan salutan alginat dan gelatin. Kekuatan mampatan meningkat kepada 1.31 MPa dan 1.08 MPa, masing-masing mewakili kenaikan 34 % dan 46 %. Bagi menghasilkan pautan kimia antara perancah  $\text{CO}_3\text{Ap}$  dan lapisan polimer, ejen silana A174 telah digunakan. Kekuatan mampatan perancah 5SA- $\text{CO}_3\text{Ap}$  dan 5BG- $\text{CO}_3\text{Ap}$  selepas dirawat meningkat sebanyak 40 % dan 35 %. Kesimpulannya, 5SA- $\text{CO}_3\text{Ap}$  yang dirawat menunjukkan kekuatan mampatan tertinggi dengan 2.17 MPa dan 52 % keliangan, yang mencukupi untuk aplikasi baik pulih tulang kanselous di mana nilai terendah bagi tulang kanselous manusia ialah > 0.15 MPa dan 50 – 90 % keliangan.

# FABRICATION AND CHARACTERIZATION OF CARBONATE APATITE SCAFFOLDS COATED WITH ALGINATE AND GELATIN

## ABSTRACT

Carbonate apatite (CO<sub>3</sub>Ap) has been received much attention in bone grafting due to similar chemical composition to human bone. However, CO<sub>3</sub>Ap artificial bone substitute still has not been commercialized due to the low thermal stability of carbonate at high temperature. Besides that, common limitation of porous materials, which is lack of strength should be taken into consideration. The aim of the present study is to fabricate CO<sub>3</sub>Ap scaffold using dissolution-precipitation reaction during hydrothermal treatment and to improve the compressive strength of scaffold by using natural polymer coating. Effect of two different solutions, which is NaHCO<sub>3</sub> and Na<sub>2</sub>CO<sub>3</sub> on β-TCP scaffold prepared via dissolution-precipitation reaction was investigated. It is found that CO<sub>3</sub>Ap scaffold with 8.95 wt.% carbonate content were successfully fabricated by NaHCO<sub>3</sub> solution. The average pore size of the scaffold is approximately 180 μm with 72% porosity. The average compressive strength obtained of CO<sub>3</sub>Ap scaffold was 0.7 MPa. Coating of CO<sub>3</sub>Ap scaffold with alginate and gelatin was performed. Compressive strength was increased up to 1.31 MPa and 1.08 MPa, which represent 34% and 46% increment, respectively. In order to make chemical link between CO<sub>3</sub>Ap scaffold and coating, silane coupling agent A174 was used. Compressive strength of the 5SA-CO<sub>3</sub>Ap and 5BG-CO<sub>3</sub>Ap scaffold after treated with silane improved by 40% and 35%, respectively. In conclusion, treated 5SA-CO<sub>3</sub>Ap shows the highest strength with 2.17 MPa and 52% in porosity is sufficient for application of cancellous bone repair where the lowest bound for human cancellous bone is > 0.15 MPa and 50 – 90 % in porosity.

# CHAPTER 1

## INTRODUCTION

### 1.1 Background of study

Tissue engineering as a new discipline has made very rapid advances since late 1980s (Min, 2006). Tissue engineering evolved from the field of biomaterials development and refers to the practice of combining scaffolds, cells, and biologically active molecules into functional tissues (Keane and Badylak, 2014). Development of biomaterial research area for bone repair in the field of tissue engineering driven by the increasing of economic burden associated with bone injury and disease. The goal of tissue engineering is to assemble functional constructs that restore, maintain, or improve damaged tissues or whole organs. Scaffolding materials are mostly used either as a carrier or template for implant bone cell or other agents or to induce the formation of bone from the surrounding tissue. Challenges are set by the design and fabrication on the synthetic tissue scaffold and the engineering of tissue constructs in vitro and in vivo. To serve as a scaffold, the materials must be biocompatible, osteoconductive, and osteointegrative, and have enough mechanical strength to provide structural support during the bone growth and remodeling (Burg et al., 2000).

Biodegradability and biocompatibility are considered important for materials to be used in tissue engineering applications. A variety of bioceramic materials such as alumina, bio-glass, hydroxyapatite (HAp), and calcium phosphates have been used to fabricate bioceramics porous scaffold. HAp,  $(Ca_{10}(PO_4)_6(OH)_2)$  and calcium phosphate  $(Ca_3(PO_4)_2)$  are among the most widely used materials for bone tissue application due to their excellent biocompatibility, osteoconductivity, and various degrees of biodegradation (Dorozhkin, 2010). The biodegradable rate should match

with the rate of new tissue formation; *in vitro* and *in vivo*. Biocompatibility has been defined as ability of scaffold to enable cell attachment, differentiation, and proliferation. Although HAp showed excellent tissue response and good osteoconductivity, HAp cannot be resorbed by osteoclasts when implanted since sintered HAp demonstrates high crystallinity (Ahmad et al., 2012). Therefore, carbonate apatite (CO<sub>3</sub>Ap), which has similar crystallinity and chemical composition to human bone has received much attention. However, artificial CO<sub>3</sub>Ap bone substitute still has not been commercialized due to certain limitations. For example, CO<sub>3</sub>Ap is unstable at high temperature above 600°C during the sintering process, due to the presence of carbonate as reported by Zaman et al. (2008).

An alternative method was proposed to fabricate CO<sub>3</sub>Ap scaffold by using dissolution-precipitation reaction during hydrothermal treatment. Alpha-tricalcium phosphate ( $\alpha$ -TCP) powder is commonly used as a precursor to fabricate the CO<sub>3</sub>Ap scaffold.  $\alpha$ -TCP is preferred to be used due to its high solubility property. Limited studies have been done on beta-tricalcium phosphate ( $\beta$ -TCP; Ca<sub>3</sub>(PO<sub>4</sub>)<sub>2</sub>) as a precursor. This is due to the lower solubility of  $\beta$ -TCP. That means, longer transformation time is required to obtain single phase of apatite. However,  $\beta$ -TCP showed added advantages where it exhibits higher mechanical strength compared to  $\alpha$ -TCP as reported by Ahmad et al. (2012). Apart from that, the cost of  $\beta$ -TCP powder is 7 times lower than that of  $\alpha$ -TCP powder.

The main advantage of inorganic scaffolds made up of HAp, bioactive glass or other bioceramics is their high biocompatibility. However, they are suffered from low mechanical strength and high brittleness as reported by Mohamad Yunus et al. (2008). Hence polymer coated ceramic framework method has been suggested to overcome this shortcoming. The polymer is not only coated at the surface but is also made to

penetrate and infiltrate the pore walls of the scaffold via remaining porosity and microcracks. In the case of polymer coating, sodium alginate and bovine gelatin are two examples of biocompatible and biodegradation polymers being developed in medicine and pharmaceutical applications.

When introducing the polymer coating, it is important to understand the fundamental driving forces which can initiate the development of adhesion strength between polymers to the ceramic scaffold. Many polymeric materials inherently have a low surface energy that results in poor surface adhesion or even complete adhesion failure. This makes difficult for coating materials to properly wet-out and adheres to the surface to these substrates. Proper surface preparation of these materials will increase surface energy, improve surface adhesion properties, and add value to the product and the process. Silanization is one of the surface treatments that commonly used to form a bond across the interface between mineral components and organic components (Joughehdoust et al., 2011).

## **1.2 Problem statement**

Mechanisms of the replacement of autograft to new bone are explained by bone remodeling process. In short, old bone is resorbed by osteoclasts and new bone is formed by the osteoblasts. Bioactive materials of  $\text{CO}_3\text{Ap}$  are expected to be an ideal bone replacement because it shows excellent osteoconductivity and cell-mediated resorbability in bone defects (Sugiura et al., 2015). Although bone apatite contains 4 - 8 wt. % of carbonate (Maruta et al., 2011; Nomura et al., 2014), sintered hydroxyapatite free from carbonate has been used as artificial bone substitute since  $\text{CO}_3\text{Ap}$  cannot be sintered due to the thermal decomposition at high temperature required for sintering. Thus, two-step fabrication of  $\text{CO}_3\text{Ap}$  scaffold or block have

been proposed. First step is the fabrication of a precursor block such as calcium carbonate and tricalcium phosphate. Then the precursors block is immersed in carbonate solution for the fabrication of  $\text{CO}_3\text{Ap}$ . Based on the dissolution-precipitation reaction, the composition of the precursor is transformed to  $\text{CO}_3\text{Ap}$ .

In the transformation to  $\text{CO}_3\text{Ap}$ , the choice of the main precursor used is important. The precursor should contain at least one component of the  $\text{CO}_3\text{Ap}$  since the solution need to be saturated with respect to the  $\text{CO}_3\text{Ap}$  based on the dissolution of the precursor. Calcium carbonate,  $\text{CaCO}_3$ , is one of the ideal precursor since it has both calcium and carbonate. However, high temperature is required for the fabrication of porous  $\text{CO}_3\text{Ap}$  using a porogen since porogen will burn out at high temperature. Various calcium phosphate, such as  $\alpha$ -TCP and  $\beta$ -TCP can be used as a precursor for the fabrication of  $\text{CO}_3\text{Ap}$  since it has suitable solubility (Ishikawa, 2016). If the solubility is too high, precipitation will not occur and thus  $\text{CO}_3\text{Ap}$  powder will be fabricated instead of  $\text{CO}_3\text{Ap}$  scaffold. Compared to  $\beta$ -TCP,  $\alpha$ -TCP is preferred because of high solubility. However,  $\beta$ -TCP has shown additional benefits where it has higher mechanical strength than  $\alpha$ -TCP (Ahmad et al., 2012).

One of the key challenges in designing tissue engineering scaffold is the required mechanical properties, e.g. the strength of the scaffold should be sufficient to provide mechanical stability in load-bearing sites prior to regeneration of new tissue. One approach to strengthen the mechanical strength of the porous scaffold is to coat with a polymer layer (Mohamad Yunos et al., 2008). Therefore, natural polymers like sodium alginate and bovine gelatin layer are used to coat the porous  $\text{CO}_3\text{Ap}$  scaffold. Because of their advantages, these natural polymers were chosen and reported to be biodegradable, biocompatible, non-toxic and abundant (Venkatesan et al., 2014).

According to Mohamad Yunos et al. (2008), the addition of polymer phase might have extra functions, e.g. the biodegradable polymer can act as a carrier for biomolecules, growth factors, and antibiotics, hence increasing the capability of tissue engineering constructs.

The concern in polymer ceramic based scaffold are the dispersion of polymer and interfacial adhesion between ceramic and polymer layer since these influence the mechanical properties (Rakmae et al., 2012). The dissimilarities between ceramic and polymer solution will cause weak interfacial adhesion. The adhesion of natural polymer to the scaffold can be enhanced by introducing the coupling agent on the scaffold. Coupling agents were used to improve the bond strength between ceramic scaffolds and the surrounding polymeric coating (Joughehdoust et al., 2011). In short, it will improve the resistance to degradation of bonds between dissimilar materials by making a chemical bridge between them. As reported by Cisneros-Pineda et al. (2014), adhesion between HAp and PMMA was improved by using 3-(trimethoxysilyl) propyl metacrylate as a coupling agent, which result in high compressive tests.

### **1.3 Objectives**

The main objective of the presents study is to develop CO<sub>3</sub>Ap scaffold as a template and coated with a natural polymer in order to improve the performance. In order to achieve the main target, the specific objectives are as follows:

- i. To investigate the effect of different solution and soaking time used in hydrothermal treatment on the transformation of  $\beta$ -TCP to CO<sub>3</sub>Ap scaffold.
- ii. To identify the effect of different concentration of sodium alginate and bovine gelatin coatings on the compressive strength of CO<sub>3</sub>Ap scaffold.

- iii. To compare the compressive strength of sodium alginate and bovine gelatin coated silane treated CO<sub>3</sub>Ap scaffold and untreated CO<sub>3</sub>Ap scaffold.

#### **1.4 Organization of thesis**

**Chapter 1** starts with a brief introduction of tissue engineering. This chapter also includes some of the problems statement for bone graft. The objectives of the research project are described in this chapter.

**Chapter 2** starts with the introduction to tissue engineering and brief insight of bone graft. It followed by the carbonate apatite for bone scaffold replacement and bioceramics scaffold that should mimic the bone composition.

**Chapter 3** describes the overall research flow in the present study, followed by materials used in the experiment and experimental procedures. The characterization methods are also discussed in this chapter.

**Chapter 4** reports the characterization of raw materials used in the preparation of scaffold. The first stages discussed on the fabrication of CO<sub>3</sub>Ap scaffold. In this stage, there are two parts involved which are the fabrication of  $\beta$ -TCP scaffold and the phase transformation reaction of  $\beta$ -TCP scaffold in carbonate solution. Hence, the effect of type of solution and soaking time on the  $\beta$ -TCP scaffold were studied. The second stage is followed by the sodium alginate and bovine gelatin coating on the CO<sub>3</sub>Ap scaffold. The study is continued by studying the effects of different concentration of polymer solution used. The concentration of polymer solution was varied from 1, 3 and 5 wt. %. Moreover, in the last stage, the silane based coupling agent known as 3-(trimethoxysilyl) propyl methacrylate (MTMS) or A174 was chosen in order to improve the interfacial adhesion between CO<sub>3</sub>Ap scaffold and polymer coating.

Comparison of properties of the treated  $\text{CO}_3\text{Ap}$  scaffold with untreated  $\text{CO}_3\text{Ap}$  scaffold were conducted.

**Chapter 5** presents the conclusion from this research and also some recommendations for future studies in this related field.

## **CHAPTER 2**

### **LITERATURE REVIEW**

#### **2.1 Introduction**

This research work focuses on the fabrication of bone scaffold as the alternative to tissue transplantation for orthopedic injury treatment. In order to produce a scaffold, this chapter starts with the introduction of tissue engineering and brief insight of bone graft. Then followed by information on carbonate apatite for bone scaffold replacement and bioceramics scaffold that should mimic the bone composition.

#### **2.2 Tissue engineering**

Tissue engineering evolved from the field of biomaterials development and refers to the practice of combining scaffold, cells, and biologically active molecules into functional tissue (Keane and Badylak, 2014). Powerful developments in the multidisciplinary field of tissue engineering have yielded a novel set of tissue replacement parts and implementation strategies. Scientific advances in biomaterials, stem cells, growth and differentiation factors, and biomimetic environments have created unique opportunities to fabricate tissues in the laboratory from combinations of engineered extracellular matrices (“scaffolds”), cells, and biologically active molecules. Scaffolding is among the major challenges faced by tissue engineering, which is the need for more complex functionality, as well as both functional and biomechanical stability in laboratory grown tissues destined for transplantation. The continued success of tissue engineering and the eventual development of true human replacement parts will grow from the convergence of engineering and basic research advances in tissues, matrices, growth factors, stem cells, and developmental biology, as well as materials science and biomaterials.

In bone tissue engineering, a scaffold is used either to induce the formation of new bone from surrounding tissue or to act as a template for implanted bone cells. The tissue engineering process involved the seeding of cells onto a scaffold. The scaffold was then cultured *in vitro* to form the matured tissue. Then it will fix into the body damaged parts such as fractured bone, cartilage or skin as an implant. The regeneration process of natural tissue will take place within the scaffold, which the blood vessels infiltrate the structure. The scaffold will degrade slowly while a newly tissue will form. This process was explained schematically in Figure 2.1 (Nainar et al., 2014).

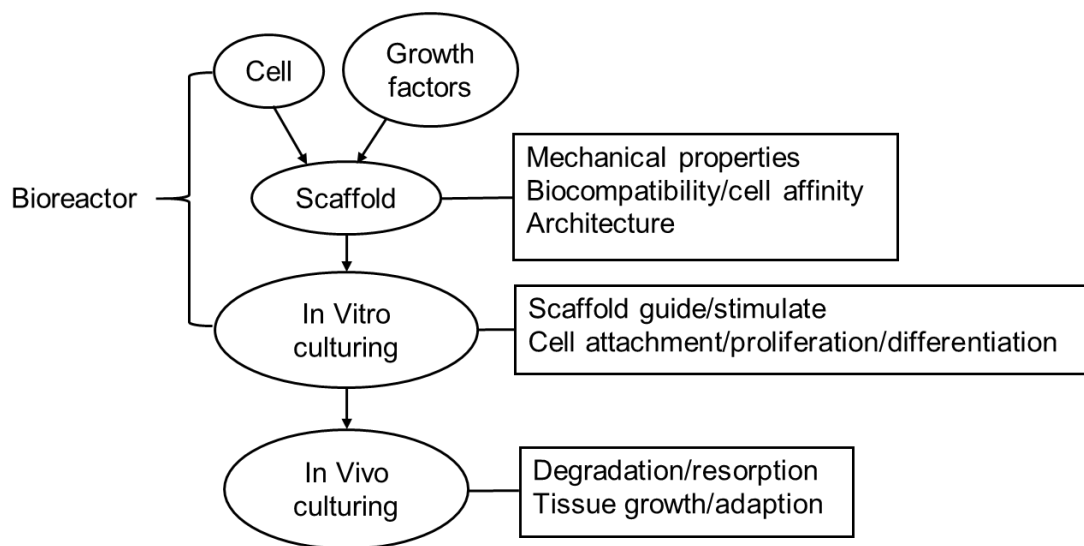


Figure 2.1 General concept of tissue engineering process

(Nainar et al., 2014)

### 2.3 Overview of bone graft

Bone grafting is a very old surgical technique. Vittorio Putti has been recognized as one of the founders of orthopedic science. The first report of the bone implant was performed in the year of 1668 (Hung, 2012). The definition of bone grafting is a surgical procedure that replaces missing bone in order to repair bone fractures that are extremely complex, pose a significant health risk to the patient, or

fail to heal properly (Donati et al., 2007). Bone grafts are implanted materials that support or promote bone healing through an osteoconduction, osteoinduction and osteogenesis mechanism to the local site. These term can be explained as below:

- **Osteoconduction**

Occurs when the bone graft material serves as a structural framework or scaffold for new bone growth that is perpetuated by the native bone (Hung, 2012). The bone forming cells in the grafting area will move across a scaffold and slowly replace it with new bone over time.

- **Osteoinduction**

The formation of new bone by stem cells transforming into osteocompetent cell by bone morphogenetic proteins (Chróścicka et al., 2016). A bone graft material that is osteoconductive and osteoinductive will not only serve as a scaffold for currently existing osteoblasts but will also trigger the formation of new osteoblasts, theoretically promoting faster integration of the graft.

- **Osteogenesis**

Occurs when vital osteoblasts originating from the bone graft material contribute to new bone growth (Karageorgiou and Kaplan, 2005). For any bone grafting procedure to be successful, the graft site must contain a sufficient number of bone-forming (osteogenic) cells to form new bone and remodel the residual graft into viable bone. For example, cancellous autograft, derived from the iliac crest or tibial plateau, contains enough cells to be considered osteogenic. Local bone from the primary surgical site generally contains cortical bone with much fewer cells.

The two major bone graft techniques are autograft and allograft. Autograft known as “gold standard” in bone substitution because it is proven, predictable, and reliable (Campana et al., 2014). In addition, it has advantages that are osteogenic, osteoinductive, osteoconductive and there is less risk of graft rejection. Autograft bone grafting involves utilizing bone obtained from the same individual receiving the graft, where the bone is harvested from the body of the patient in the first place. Bone can be harvested from non-essential bones such as fibula, the chin, the rib and even parts of the skull. In autograft, donor site morbidity that is damage of remaining tissue at the site of harvest is a major limitation. Besides this, limited availability and unpredictable resorption characteristics of the bone are also matters of concern.

Allograft bone grafting is like autograft, which is derived from human. The different is that allograft is harvested from an individual other than the patient’s body (Hung, 2012). For allograft, the bone is taken from cadavers that donated their bone so that it can be used for living people who need it. Usually, this typical source of bone come from a bone bank. The advantages of allograft are osteointegrative and osteoconductive and may exhibit osteoinductive potential, but it is not osteogenic because it contains no live cellular components. Besides this, allograft has a major limitation, which is the possibility of immune-rejection from the host body and increase the chances of disease transmission. Both of these two techniques come along with serious concerns and limitations (Mallick et al., 2015). As an alternative, bone graft substitute is increasingly used especially in oncologic surgery, traumatology, revision prosthetic surgery and spine surgery (Campana et al., 2014).

Bone graft substitute involves the extensive use of porous scaffolds to provide the extracellular environment for the regeneration of bone tissues. These scaffolds are the main ingredient for bone tissue engineering. It will serve as a template and can be

used to guide bone regeneration and repair defects to enhance bone regeneration (Nainar et al., 2014). In addition, scaffolds are used as bone grafting in order to replace the tissue damaged due to accident, trauma or any disease. The concept of bone regeneration by bone scaffold substitute is shown in Figure 2.2. The scaffolds are implanted into an injured site. The regeneration of tissue or organs will occur with the combination of cells, signals, and scaffold itself. Type of material is one of the important factors that need to be considered in the fabrication of porous scaffold. The material should meet the demands of tissue engineering, such as biocompatibility.

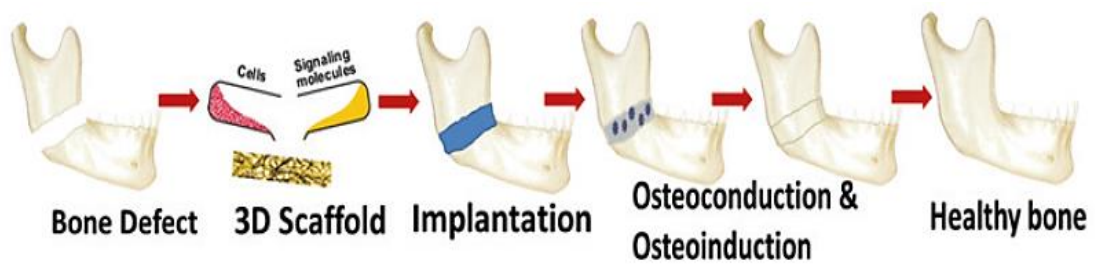


Figure 2.2 Concept of bone regeneration by bone scaffold substitute  
(Mohamed and Shamaz, 2015)

The evolution of bone graft substitute can be divided into three generations. The first generation includes the usage of metals such as stainless steel, titanium, and alloys; ceramics such as alumina and zirconia; and a polymer such as silicone rubber and polypropylene. However, it occurs a non-specific immune response to a material that cannot be phagocytosed, in which an inflammatory response persists until the foreign body becomes encapsulated by fibrotic connective tissue, shielding it from the immune system and isolating it from the surrounding tissues. To avoid this non-specific immune response, second-generation bone graft substitutes were developed with bioactive interfaces which would elicit a specific biological response (i.e., osteoconduction). The second generation was developed by introducing the coating

layer on the first generation. The bioactive ceramics like HAp and biodegradable polymers were used. The aim of the second generation is to match the rate of degradation with a healing rate of the injured bone tissue. The third generation is followed by inducing specific cellular responses on integrating the bioactivity and biodegradability of the second generation. The summary of bone graft evolution is shown in Figure 2.3.

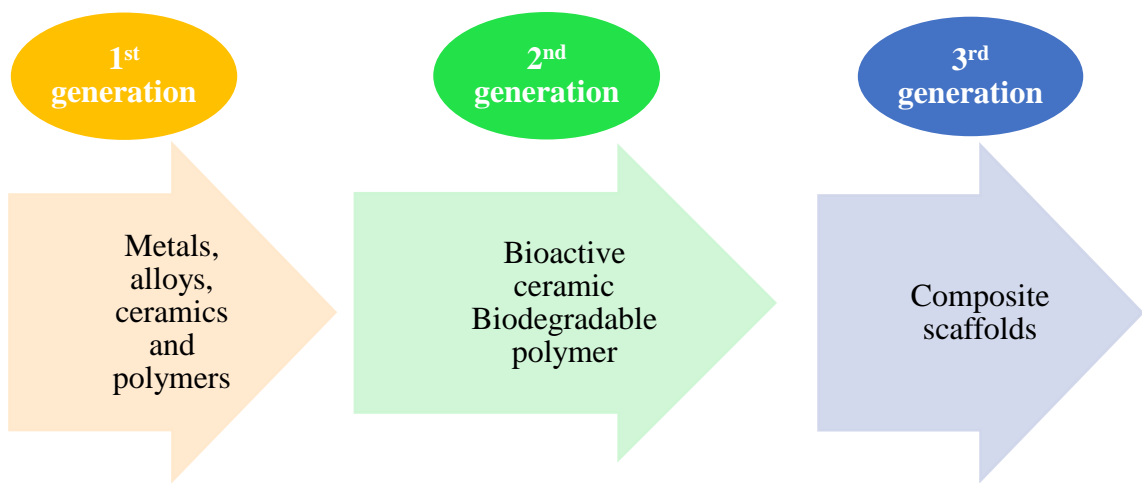


Figure 2.3 Evolution of bone graft substitute materials  
(Polo-Corrales et al., 2014)

#### 2.4 Carbonate apatite bone replacement

Bioactive materials like carbonate apatite, ( $\text{CO}_3\text{Ap}$ ) are expected to be an ideal bone replacement because it shows excellent osteoconductivity and cell-mediated resorbability in bone defects (Sugiura et al., 2015). The dominant inorganic component of bone is  $\text{CO}_3\text{Ap}$  that contains 4 – 8 wt. % of carbonate (Zaman et al., 2008; Maruta et al., 2011; Nomura et al., 2014). The presence of carbonate in the apatite lattice contributed to the ease of resorption in bony tissue (Doi et al., 1998). That means  $\text{CO}_3\text{Ap}$  is better than HAp in biological response as bone substitute materials.  $\text{CO}_3\text{Ap}$  can be denoted as two types; A-type or B-type. This is due to the basis of the

substitution site of carbonate ions in the apatitic lattice. The comparison of these two types of CO<sub>3</sub>Ap is shown in Table 2.1. However, B-type CO<sub>3</sub>Ap is a candidate for an artificial bone substitute since its structure and crystallinity are similar to natural bone.

Table 2.1 Comparison of A-type and B-type of CO<sub>3</sub>Ap (Tsuru et al., 2017)

<b>A-type</b>	<b>B-type</b>
<ul style="list-style-type: none"> <li>• CO<sub>3</sub> for OH substitution</li> <li>• Can be prepared at high temperature</li> <li>• Found in the old tissue</li> </ul>	<ul style="list-style-type: none"> <li>• CO<sub>3</sub> for PO<sub>4</sub> substitution</li> <li>• Can be prepared by precipitation or by hydrolysis at a low temperature</li> <li>• Found in the young tissue</li> </ul>

To date, artificial CO<sub>3</sub>Ap bone substitute still has not been commercialized. This is due to the low thermal stability of carbonate at high temperature, where CO<sub>3</sub>Ap decomposes at temperature 400°C and the pronounced thermal decomposition occurs at 600 – 700°C (Nomura et al., 2014). An alternative method was proposed to fabricate CO<sub>3</sub>Ap scaffold using dissolution–precipitation reaction during hydrothermal treatment (Almirall et al., 2004; Wakae et al., 2008; Maruta et al., 2011; Tsuru et al., 2017). Apart of hydrothermal treatment, other methods such as carbonation (Cahyanto et al., 2016), phosphorization (Zaman et al., 2008) and hydrolysis (Pieters et al., 2010) were also reported able to fabricate CO<sub>3</sub>Ap.

#### 2.4.1 Hydrothermal treatment

An alternative method to fabricate CO<sub>3</sub>Ap block or scaffolds by dissolution-precipitation reaction during hydrothermal treatment was widely used since 2007 (Wakae et al., 2007). In this method, selecting a suitable precursor plays an important factor based on their chemical and physical properties. The precursor should not

disintegrate in the solution and must contain at least one component of CO<sub>3</sub>Ap such as calcium (Ca), phosphate (P) or carbonate (CO<sub>3</sub>) (Ishikawa, 2016). For example, the precursors used in previous works are varied using calcite (CaCO<sub>3</sub>) (Zaman et al., 2008), gypsum (Nomura et al., 2014), calcium hydrogen phosphate dehydrate (DCPA) (Tsuru et al., 2017) and alpha-tricalcium phosphate ( $\alpha$ -TCP) (Wakae et al., 2008; Tsuru et al., 2013; Sugiura et al., 2015). Table 2.2 summarizes the precursor used by previous researchers to fabricate CO<sub>3</sub>Ap scaffold by hydrothermal treatment.

Table 2.2 Types of precursor used in the fabrication of CO<sub>3</sub>Ap scaffold by hydrothermal treatment

<b>Year</b>	<b>Precursors</b>	<b>Carbonate source</b>	<b>References</b>
<b>2017</b>	DCPA block	Sodium hydrogen carbonate Sodium carbonate	(Tsuru et al., 2017)
<b>2015</b>	$\alpha$ -TCP foam	Sodium hydrogen carbonate	(Sugiura et al., 2015)
<b>2014</b>	Gypsum	Disodium hydrogen phosphate Disodium hydrogen carbonate	(Nomura et al., 2014)
<b>2013</b>	- $\alpha$ -TCP scaffold - $\beta$ -TCP scaffold (from heat treatment of $\alpha$ -TCP scaffold)	Disodium carbonate solution	(Tsuru et al., 2013)
<b>2008</b>	Gypsum-calcite composite	Ammonium phosphate	(Zaman et al., 2008)
<b>2007</b>	$\alpha$ -TCP foam	Ammonium carbonate	(Wakae et al., 2007)

Based on Table 2.2, the  $\alpha$ -TCP powder is commonly used as a precursor to fabricate the CO<sub>3</sub>Ap scaffold.  $\alpha$ -TCP is preferred due to its high solubility. Kanji et al. (2013) reported that high solubility of  $\alpha$ -TCP in aqueous carbonate solution will

accelerate the formation of nuclei site and quickly transform to  $\text{CO}_3\text{Ap}$ . Wakae et al. (2008) also used  $\alpha$ -TCP foam as a precursor in their research, where  $\alpha$ -TCP foam was immersed in 4 mol/L sodium carbonate ( $\text{Na}_2\text{CO}_3$ ) at  $100^\circ\text{C}$  and  $200^\circ\text{C}$  for various periods up to 72 hours. Plate-like crystal obtained after the treatment at  $200^\circ\text{C}$  had a smooth surface whereas the crystal obtained after the treatment at  $100^\circ\text{C}$  were constructed from spherical particles. Figure 2.4 shows the example of a crystal formed on the scaffold after hydrothermal treatment. Based on their results, it was concluded that the crystals morphology of the surfaces is governed by the hydrothermal treatment temperature.

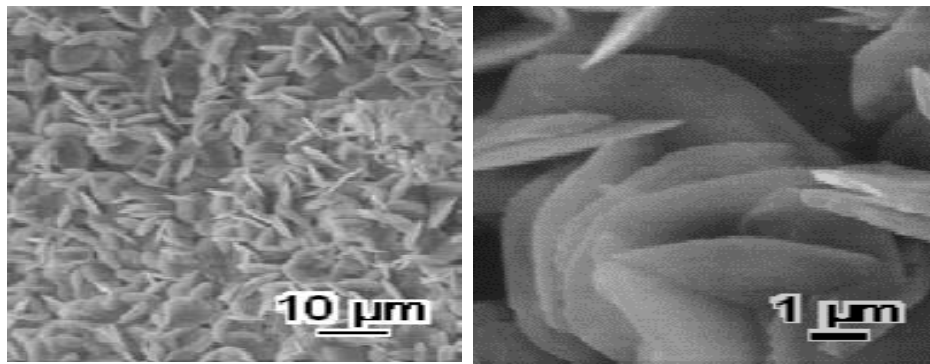
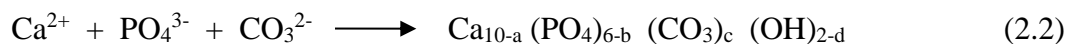


Figure 2.4 Scanning Electron Microscopy (SEM) image of  $\alpha$ -TCP foam after immersion in 4 mol/L  $\text{Na}_2\text{CO}_3$  at  $200^\circ\text{C}$  (Wakae et al., 2008)

During hydrothermal treatment, the dissolution–precipitation reaction occurs. For example,  $\text{CO}_3\text{Ap}$  foam can be fabricated from  $\alpha$ -TCP precursors as shown in equations 2.1 and 2.2.



Dissolution of  $\alpha$ -TCP results in the release of  $\text{Ca}^{2+}$  and  $\text{PO}_4^{3-}$  ions into the solution (equation 2.1). When  $\alpha$ -TCP soaked in the solution contain  $\text{CO}_3^{2-}$  ion, the solution is

supersaturated with respect to  $\text{CO}_3\text{Ap}$ . Thus,  $\text{Ca}^{2+}$ ,  $\text{PO}_4^{3-}$  and  $\text{CO}_3^{2-}$  will be precipitated on the surface of foam as  $\text{CO}_3\text{Ap}$  as reported by Ishikawa et al. (2016). The example mechanisms of dissolution-precipitation ions are shown in Figure 2.5.

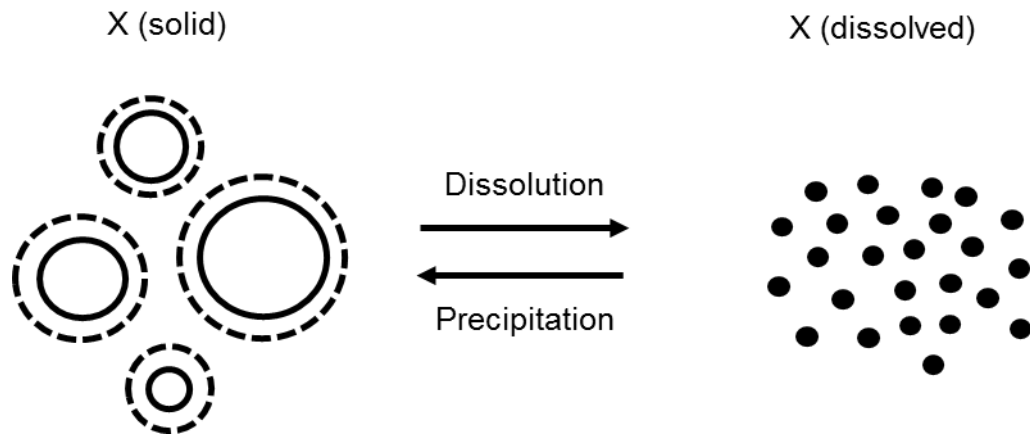


Figure 2.5 Mechanisms of dissolution-precipitation ions (Willmann et al., 2012)

Another work by Wakae et al. (2008), investigated the effect of different concentration of ammonium carbonate  $(\text{NH}_4)_2\text{CO}_3$  solution at  $200^\circ\text{C}$  for 24 hours. After treatment in different solutions concentration, crystals of different morphology were observed. Sugiura et al. (2015) investigated the setting reaction of  $\alpha$ -TCP foam granules in the carbonate salt solution. Different concentrations of sodium hydrogen carbonate ( $\text{NaHCO}_3$ ) solution was used in their treatment. Treatment at higher concentration of  $\text{NaHCO}_3$  solution results in increased  $\text{CO}_3$  content in the apatitic structure and the morphology observed changed from fiber-like to plate-like with small aspect ratio. It is observed that the surface characteristics are also governed by the type and concentration of the solution used. When treated with  $\text{Na}_2\text{CO}_3$  and  $\text{NaHCO}_3$ , the crystal morphology changes to plate-like crystals. In contrast, the structure of the crystal changed to needle-like when immersed in  $(\text{NH}_4)_2\text{CO}_3$ .

### **2.4.2 Carbonation and phosphorization**

According to Barralet et al. (2003), the carbonation process was performed by flowing carbon dioxide (CO<sub>2</sub>) gas during the sintering or treatment process. B-type carbonate apatite from apatite cement (AC) was prepared by Cahyanto et al. (2016). First, the AC powder was prepared. After that, AC powder was mixed at a specific ratio with distilled water while being packed into Teflon mold and placed with the 100% CO<sub>2</sub> gas supply in the incubator. In this process, the solution would be saturated with respect to CO<sub>3</sub>Ap, since CO<sub>3</sub><sup>2-</sup> ions from CO<sub>2</sub> gas exist in the body environment, the following carbonation process may occur based on the dissolution–precipitation reactions as previously mentioned.

It should be highlighted that the CO<sub>3</sub>Ap need to be fabricated from precursor's materials through phase conversion via hydrothermal or solution mediated dissolution–precipitation treatment. The first step is the fabrication of precursors and the second step is immersed in a solution in which missing elements for the fabrication of CO<sub>3</sub>Ap. In the phosphorization process, the basic concept based on the dissolution–precipitation reaction was applied by immersing the precursors in a phosphate salt solution (Zaman et al., 2008). For example, Maruta et al. (2011) have been prepared low–crystalline of CO<sub>3</sub>Ap foam based on phase transformation of calcite (CaCO<sub>3</sub>) in disodium hydrogen phosphate (Na<sub>2</sub>HPO<sub>4</sub>). Based on their finding, CaCO<sub>3</sub> foam was successfully transform to CO<sub>3</sub>Ap after immersion in Na<sub>2</sub>HPO<sub>4</sub> solution at 60°C for 2 weeks without changing its macroscopic structure of the foam.

### **2.5 Bioceramic scaffold**

Scaffold design and fabrication are a major area in biomaterials research, which include important subjects for tissue engineering and regenerative research

(Dhandayuthapani et al., 2011). One of the challenges of tissue engineering is developing scaffolds that are an appropriate mimic of the natural extracellular matrix (Katti et al., 2008). To mimic the structure of bone, it is essential to understand and know the structural features of natural bone (Mallick et al., 2015). When developing the porous structures of the scaffold, some criteria must be considered, namely porosity and pore size, mechanical competence, biodegradable characterization, surface properties, and biocompatibility. These requirements can be explained as follows:

**i. Porosity**

An ideal scaffold would favor porosity with 50 – 90 % as reported by Ferreira et al. (2012). Although porosity does not play a significant role in cell attachment but with the increased in porosity will allow space transport of oxygen and other nutrients (Mallick et al., 2015).

**ii. Pore Size**

Interconnected pores play an important factor in the fabrication of scaffold. The interconnected pores will allow the flow of nutrients and for cell growth (Eisenbarth, 2007). Pore size between 300 and 500  $\mu\text{m}$  is suitable for cell penetration, tissue in-growth, and vascularization (Mohamad Yunus et al., 2008). For example, Teixeira et al. (2009) produced a scaffold with a pore diameter ranging from 100 to 400  $\mu\text{m}$ , where the pore size of over 300  $\mu\text{m}$  is favorable for the bone formation and regeneration as reported by Woottichaiwat et al. (2011). While Karageorgiou et al. (2005) suggested that pore size should be  $\geq 100 \mu\text{m}$  for the proper regeneration of mineralized bone.

### **iii. Mechanical Properties**

According to Woottichaiwat et al. (2011), the strength of the scaffold should be sufficient enough to provide mechanical stability in load-bearing sites prior to the regeneration of new tissue. Li et al. (2015) reported in their article that the lower bound of the values for human cancellous bone is  $> 0.15$  MPa and  $\approx 90$  % for porosity. It is also important to retain mechanical strength after the implantation for hard load-bearing, such as bone and cartilage.

### **iv. Biodegradable**

The type of materials used governs biodegradability. The materials should be biodegradable in nature. The biodegradable rate should match to the rate of new tissue formation, *in vitro* and *in vivo*. Calcium phosphates, including hydroxyapatite (HAp) and tricalcium phosphate (TCP), are among the most widely used materials for bone tissue application (Teixeira et al., 2009) due to their excellent biocompatibility, osteoconductivity and various degrees of biodegradation (Huang and Miao, 2007).

### **v. Biocompatibility**

One of the primary requirement of the scaffold is biocompatibility. Biocompatibility of a scaffold is described as its ability to perform appropriate host responses in a specific application and non-toxic on biological systems (Bose et al., 2012).

There are various methods that can be used to produce the porous bioceramic scaffold including a polymeric sponge method (Etal et al., 1963; Miao et al., 2007; Teixeira et al., 2009; Sopyan and Kaur 2009; Mohammad Saman and Jaafar 2015), freeze casting (Deville et al., 2006; Fu et al., 2008), gel casting (Pilar et al., 2000;

Bezzi et al., 2003; Dash et al., 2015), and direct foaming (Almirall et al., 2004; Silva et al., 2007). The oldest scaffold fabrication of ceramics by the polymeric sponge method or replication method dates back to the early 1960s. Karl and co-workers in 1963 were the first research group used a polymeric sponge as a template to produce the porous ceramic structure (Pilar et al., 2000). This method is safe and easy to produce (Mohamad Yunos et al., 2008; Dash et al., 2015). Furthermore, this is the most common method used since the prepared scaffold has a controllable pore size, interconnected pores, and desired geometry, but is poor in mechanical strength (Ramay and Zhang, 2003).

Miao et al. (2007) have produced a porous calcium phosphate ceramic (CPC) with the interconnected macropores ( $\sim 1$  mm) and micropores ( $\sim 5$   $\mu\text{m}$ ) as well as high porosity ( $\sim 80$  %) by burning polyurethane foams (PU) at  $600^\circ\text{C}$  and then firing the coated PU foams with calcium phosphate cement at  $1200^\circ\text{C}$  for 2 hours. Sopyan et al. (2009) have also used a polymeric sponge as a template to prepare a hydroxyapatite scaffold. The template is initially soaked in the slurry (a mixture of hydroxyapatite powder, distilled water and dispersing agent at a certain ratio) until it is homogeneously coated to the template. Then the template is subsequently dried to burn out the template at the range between  $300$  to  $800^\circ\text{C}$  (Mohamad Yunos et al., 2008) followed by sintering at appropriate temperatures depending on the material for densification. The porosity is observed to be around  $34.3 - 59.8$  %. Figure 2.6 shows the schematic diagram of the polymeric sponge method.

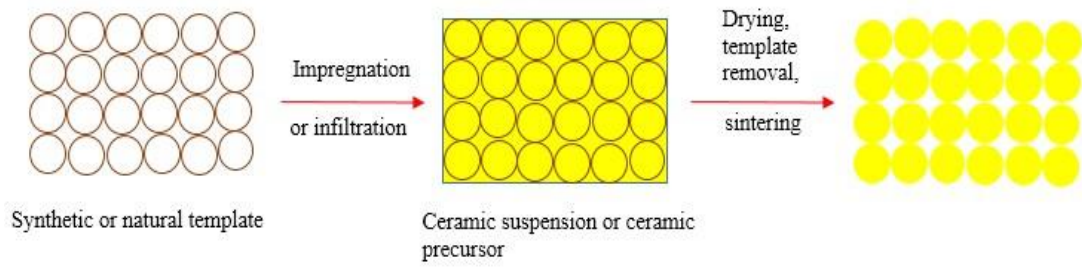


Figure 2.6 Schematic diagram of the polymeric sponge method  
(Mamat et al., 2017)

For direct foaming method, the porous structure of air bubbles was obtained from the air that was incorporated into a ceramic suspension (Mohamad Yunos et al., 2008). Alternative process foaming of ceramic slurry is done by mechanical agitation or in situ evolution of gases (Silva et al., 2007). The properties of the scaffold produced by this method are mostly similar to the gel casting, where high mechanical strength is obtained. However, non-uniform pore size distribution and poorly interconnected pores are reported ( Sepulveda et al., 2000; Ramay and Zhang, 2003). Moreover, it was possible to prepare cellular ceramic foam with different porosity, densities and pore distribution depending on the solid’s loading and additives used (Silva et al., 2007). The direct foaming method is schematically shown in Figure 2.7.

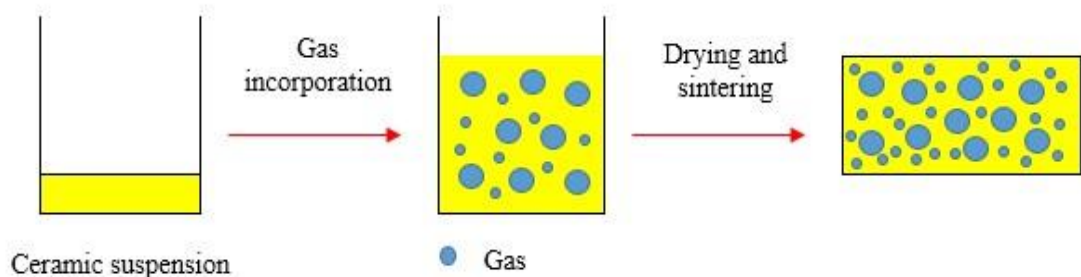


Figure 2.7 Schematic diagram of the direct foaming method (Mamat et al., 2017)

Gel casting is widely used for the processing of porous and dense ceramics (Dash et al., 2015). In 1991, Omatete and Janney were the first researchers to report on the gel casting process (Janney et al., 1998). The scaffold fabricated by using this method usually results in high mechanical strength but has non-uniform pore size distribution and poorly interconnected pores (Ramay and Zhang, 2003). The basic process involves in-situ polymerization and gelatin of organic additives, which are used along with dispersed slurry. The additives and powder loading are examples of parameters that effect on the microstructure and porosity. Sepulveda et al. (2000) used gel casting of foam to produce the porous hydroxyapatite with high porosity up to 90 % and 20 to 1000  $\mu\text{m}$  of pore interconnectivity. While on the other hand, Dash et al. (2015) used gel casting for porous hydroxyapatite, but with the addition of naphthalene as pore formers. The function of additional naphthalene is to provide an additional parameter for controlling the porosity and pore connectivity. Figure 2.8 shows the schematic diagram of the gel-casting process.

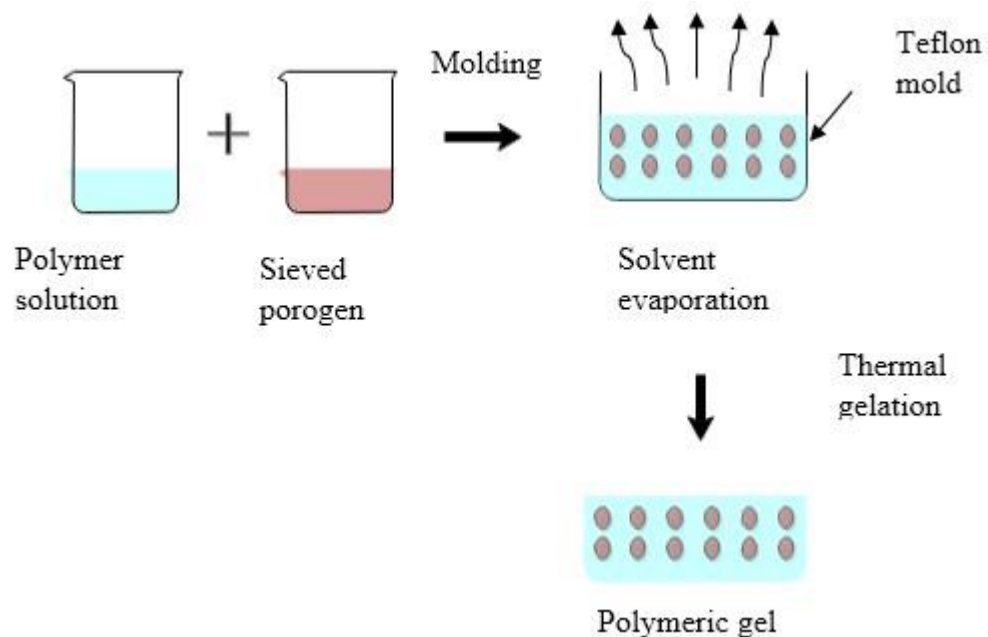


Figure 2.8 Schematic diagram of the gel-casting process (Mamat et al., 2017)

The individual method to fabricate a scaffold can also be combined to tailor the scaffold properties and also to obtain better porous structure and mechanical properties. The first report of a combination method was made by Li and co-workers (2002). The process is a combination of a foaming method and dual-phase mixing method to fabricate a macroporous scaffold where HAp slurry and poly (methyl methacrylate), (PMMA) were mixed together at the volume ratio of 1:1 (Li et al., 2002). It results in a higher porosity of 80 % and interconnected macropores (~1 mm) and micropores (~5  $\mu\text{m}$ ). While Ramay et al. (2003) combined gel-casting and polymer sponge methods to prepare a porous hydroxyapatite scaffold. In this combination method, a polymer sponge is infiltrated with a ceramic slurry that contains a monomer and initiator for rapid gelation by in-situ polymerization, resulting in increased mechanical strength and a controllable porous structure.

On the other hand, Almirall et al. (2004) also used a combination method to produce an HAp scaffold by using a combination of foaming and hydrolysis of an  $\alpha$ -TCP paste. To prepare the foam, the  $\alpha$ -TCP powder was mixed with precipitated hydroxyapatite and hydrogen peroxide ( $\text{H}_2\text{O}_2$ ) that acts as a foaming agent at different concentrations. After mixing, the paste was poured into the Teflon molds and kept at  $60^\circ\text{C}$  for 2 hours for decomposition of hydrogen peroxide at this temperature. This was followed with immersion in Ringer's solution at various periods of time. Based on the result, it can be concluded that a scaffold that combines interconnected macroporosity with a high microporosity can be obtained at low temperature by the foaming of an  $\alpha$ -TCP paste and subsequent hydrolysis.

Huang et al. (2007) used  $\text{H}_2\text{O}_2$  as a foaming agent. They combined the  $\text{H}_2\text{O}_2$  with a PU sponge to produce HAp scaffold. PU foams as the template was dipped into the slurry and fired to remove the PU foam. Then, the remaining green template were